Some Effects of Different Cloud Parameterizations in a Mesoscale Model and a Chemistry Transport Model

NICOLE MÖLDERS,† HEINZ HASS,* HERMANN J. JAKOBS,* MANFRED LAUBE, AND ADOLF EBEL

Universität zu Köln, Institut für Geophysik und Meteorologie, EURAD, Köln, Germany

(Manuscript received 23 September 1992, in final form 17 September 1993)

ABSTRACT

Chemistry transport models often ignore the cloud parameters that can be provided by meteorological preprocessors like mesoscale meteorological models. They often recalculate these parameters with algorithms that differ from those used in the meteorological preprocessors. Hence, inconsistencies can occur between the treatment of clouds in the meteorological and chemical part of the model package. In this study the influence of five different cloud parameterization schemes used in a well-known mesoscale meteorological model on the results of a stand-alone version of a cloud and scavenging module is illustrated. The differences between the results provided by five model runs with different cloud modules and those recalculated by the stand-alone version are discussed. Such differences occur due to the inconsistencies between the different cloud parameterization schemes in the meteorological model and the cloud and scavenging module. The results of the cloud and scavenging module differ due to the different meteorological input data provided by the meteorological model. It is manifested both in recalculated cloud parameters and in predicted wet deposition rates. As illustrated in this study, the rate of wet deposition strongly depends on the cloud parameterization scheme used in the meteorological model and, hence, on the model architecture itself.

1. Introduction

Clouds play an important role in the vertical redistribution, chemical transformation, and removal of trace species in the troposphere (Chang et al. 1987). Clouds also significantly alter the photolysis rates, and, hence, the gas-phase chemistry below, within, and above clouds. Therefore, improved chemistry transport models and their meteorological preprocessors demand cloud parameterization schemes that are able to calculate the effects of microphysics not only on dynamic processes, but also on vertical mixing, gas- and aqueous-phase chemistry processes, and scavenging processes.

Results from numerical simulations performed by Orville and Kopp (1977), Cotton et al. (1982), Lin et al. (1983), Dudhia (1989), Zhang (1989), and some others show that the inclusion of ice microphysics in cloud modules results in a better description of cloud and precipitation formation processes. This is due to the fact that the freezing of cloud droplets and the growth of ice crystals by water vapor deposition and riming contribute to latent heat release to enhance cloud growth, to affect the formation of precipitation, and to alter the structure of circulation fields.

In chemistry transport models the liquid water content is one of the key quantities. The distribution of a species between gas and aqueous phases in clouds is strongly affected by the degree of solubility characterized by the Henry's law constant and the liquid water content. Thus, the relative importance of gas- and aqueous-phase chemistry in clouds also depends on this quantity.

At temperatures between freezing point and −35°C or so a fraction of the condensed water is ice (Fletcher 1962); that is, supercooled water and ice coexist within this temperature range. This fraction does not contribute to aqueous chemistry because ice is commonly considered chemically conservative. Ice particles also reduce the liquid water content by water vapor deposition and riming. The latter occurs when the terminal velocities of the ice crystals are larger than those of the cloud droplets. Furthermore, raindrops and ice crystals have different shapes, sizes, densities, and, hence, terminal velocities. Therefore, the presence of ice causes changes in scavenging rates (Scott 1981; Chang 1984; Topol 1986). Raindrops and ice crystals can also evaporate in unsaturated layers, and, hence, can alter the chemical environment of these layers.

In view of these facts it is obvious that the effects of ice microphysics must be included not only in the me-

† Current affiliation: Arbeitsgruppe für Umweltmeteorologie, Garmisch-Partenkirchen, Germany.

* Current affiliation: Förderverein Rhein. Institut für Umweltforschung, c/o EURAD, Köln, Germany.

Corresponding author address: Nicole Mölders, Arbeitsgruppe für Umweltmeteorologie, Ludwigstraße 85, D-82467 Garmisch-Partenkirchen, Germany.

teorological preprocessor, but also in the chemistry transport model, where inconsistencies between the cloud modules of these model parts should be avoided.

The model package used in this study is EURAD (European Acid Deposition Model), which simulates the transport, transformation, and deposition of chemical tracers. It consists of three submodules: EEM (EURAD Emission Model), which gives the emission scenario of the gases depending upon time and location (Memmesheimer et al. 1991), MM4 (Mesoscale Model Version 4), which simulates the meteorological fields (Anthes et al. 1987), and the chemical part CTM (Chemistry Transport Model), which predicts the transport, transformation, and wet and dry deposition (Hass et al. 1990; Hass et al. 1993). CTM is based on RADM (Chang et al. 1987). The meteorological fields predicted by MM4 (temperature, pressure, wind, water vapor, rain) serve as input for the CTM.

The MM4 contains four options for the treatment of the hydrological cycle (Anthes et al. 1987) but none of them includes ice processes. In the first (dry) option, water vapor is treated as a passive variable. Excess water vapor over a critical relative humidity of RH_c (RH_c = 100% in the most simulations) is removed and the precipitation accumulated, but latent heat of condensation is not added into the thermodynamic equation. In the second option, the excess water vapor over RH_c is also removed as precipitation but the latent heat is added to the thermodynamic equation. Evaporation in unsaturated layers is not allowed. These two options are not considered in this study.

The third option is the cumulus parameterization scheme following Kuo (1974), modified by Anthes (1977). Cumuliform clouds are assumed to occur if sufficient horizontal moisture convergence and instability are present above a grid area. The fourth option is the warm scheme [often called explicit scheme (cf. Anthes et al. 1987)]. It predicts water vapor, cloud water, and rainwater and treats the warm path of precipitation formation as described in Hsie and Anthes (1984) and Anthes et al. (1987), where condensation, autoconversion, accretion, and evaporation are taken into account.

The computer performance, capacity, and storage, as well as the model architecture of EURAD do not allow us to simulate cloud microphysical and chemical processes simultaneously. So simulations of cloud dynamics are performed in MM4 and the predicted distributions of water vapor, temperature, pressure, and precipitation serve as hourly input for the CTM cloud module developed by Walcek and Taylor (1986). Some modifications on this cloud module were made by Hass et al. (1993) and Chang et al. (1987). Although neither the cumulus parameterization scheme nor the warm scheme provide any ice content, the CTM cloud module considers ice and, in a temperature range from −18°C to freezing point, the coexistence of ice and supercooled water. At temperatures below this range only ice is considered. As reported by Fletcher (1962), many authors observed supercooled cloud water up to temperatures of −33° to −41°C. In view of this temperature discrepancy, we must expect that concentration changes due to aqueous phase chemistry processes can be underestimated by the CTM cloud module.

Several reasons are responsible for the inconsistency within the EURAD model architecture concerning the treatment of clouds: RADM, on which EURAD is based, was originally conceived to be able to run with observation and rainfall data as input data. Later, MM4 and the cumulus parameterization scheme were used as meteorological preprocessors for RADM. This structure was retained in the standard version of the EURAD model. Since the cumulus parameterization scheme does not predict cloud and rainwater or ice, the CTM cloud module calculates the liquid water and ice, even in the cases where MM4 versions (e.g., MM4 with warm scheme or with the ice parameterization developed for this study) can deliver these parameters. All other cloud parameters like cloud cover, cloud top, and cloud base are also determined by the CTM cloud module to simulate aqueous-phase chemistry and vertical redistribution processes.

Within the framework of this study, an ice parameterization scheme considering the coexistence between ice and supercooled water up to temperatures of −35°C has been developed and incorporated into MM4 as a fifth option in order to obtain a better physical and dynamical representation for the simulation of European mesoscale cloud systems. This scheme is based on the warm scheme, where the treatment of the ice microphysics follows Cotton et al. (1982). The ice parameterization scheme developed for our study is described in section 2. For simplicity, only one ice class reaching from cloud ice to lightly rimed graupel was taken into account. MM4 has further been expanded to be able to run concurrently with the cumulus parameterization scheme and the warm scheme (sixth MM4 option) or with the cumulus parameterization scheme and the ice parameterization scheme (seventh MM4 option) to simulate both stratiform and cumuliform clouds.

The ice parameterization scheme of Dudhia (1989), which was also used in MM4 Zhang (1989), considers no supercooled water. As a consequence, no aqueous-phase chemistry processes can be simulated if the temperature at each cloud level is below freezing. Therefore, the ice parameterization scheme of these authors were not taken into consideration.

The aim of this study is to illustrate the influence of the inconsistency between the treatment of clouds in the meteorological preprocessor and the chemistry transport model on the diagnosed cloud parameters and on the predicted wet deposition. Furthermore, differences between the cloud parameters predicted by the cloud modules are presented and discussed. Here, the cumulus parameterization and the warm scheme as well as the three additional MM4 options mentioned

above permit study of five different cloud modules and their influence on aqueous-phase chemistry and wet deposition. As illustrated in this study, the rate of wet deposition strongly depends on the cloud parameterization scheme used in the meteorological model and, hence, on the model architecture itself.

2. Ice parameterization

Since the cumulus parameterization scheme and the warm scheme are well known from literature, this section describes only the parameterization of the warm and cold cloud processes in MM4. The condensation CD_{vc}, autoconversion CN_{cr}, accretion CL_{cr}, rainwater evaporation processes EV_{rv}, precipitation as rain, and the terminal velocity of rain v_{Tr} are treated as in the warm scheme (Hsie and Anthes 1984; Anthes et al. 1987). The saturation adjustment is based on Asai (1965). The ice-phase microphysics parameterization follows Cotton et al. (1982). It includes water vapor deposition and sublimation (CD_{vi}), cloud droplets riming onto ice crystals of different sizes (CL_{ci}), melting (ML_{ir}), sedimentation, and finally, precipitation as ice. In the following notation the subscripts v, c, r, i, and s refer to water vapor, cloud water, rainwater, ice particles, and saturation, respectively. In the case of two subscripts the first index denotes the phase that is depleted while the second subscript denotes the phase in which the water component is growing. If precipitation occurs, a single index indicates the type of precipitation. The parameter k stands for v, c, r, and i, respectively. The equation for the moisture component k is now given by

$$\frac{\partial p^* q_k}{\partial t} = -m^2\left[\frac{\partial (p^* u q_k/m)}{\partial x} + \frac{\partial (p^* v q_k/m)}{\partial y}\right] - \frac{\partial (p^* q_k \sigma^\bullet)}{\partial \sigma} + p^* M_k + D q_k - g\frac{\partial (\rho_a q_k v_{Tk})}{\partial \sigma}. \quad (1)$$

Here, p^* is the difference between the surface pressure p_s and the top of the model, $p_{100} = 100$ hPa. Furthermore, σ is vertical coordinate of the model, u and v are the horizontal components of the wind, $\sigma^\bullet$ is the vertical velocity, m is the map scale factor, ρ_a is the density of the air, v_{Tk} is the mass-weighted terminal velocity, g is the acceleration of gravity, and q_k is the mixing ratio of the phase k. The microphysical processes M_k of q_k are parameterized by the following phase transition terms:

$$M_v = EV_{rv} - CD_{vc} - CD_{vi}, \quad (2)$$

$$M_c = CD_{vc} - CN_{cr} - CL_{cr} - CL_{ci}, \quad (3)$$

$$M_r = CN_{cr} + CL_{cr} + ML_{ir} - EV_{rv}, \quad (4)$$

$$M_i = CD_{vi} + CL_{ci} - ML_{ir}, \quad (5)$$

which will be discussed in detail later. The first three terms on the right-hand side in Eq. (1) represent the transport and the fourth term represents the phase transition processes. The term D denotes the contribution of horizontal and vertical diffusion to the rate of change of phase k, and the last term represents that by sedimentation. It is assumed that in the case of ice and rainwater the effects of vertical diffusion can be neglected in comparison with the contributions by sedimentation. Furthermore, the fall velocity of cloud droplets is assumed to be zero. No distinction between cloud ice and falling ice particles are made, which means that immediately after ice has formed, it begins to sedimentate. This can result in lower cloud tops, especially at the beginning of cloud formation as the parameterization of the mean mass-weighted terminal velocity of ice considers all sizes, even the very large ones that have not been built at that time. Similar reasons account for the fact that the parameterization of the mean mass-weighted terminal velocity of raindrops overpredicts the sedimentation at the beginning of rain formation.

The hydrostatic equation is modified to take into account the mixing ratios of cloud water, rainwater, and ice:

$$\frac{\partial \Phi}{\partial \ln(\sigma + p_{100}/p^*)} = -RT_v\left(1 + \frac{q_c + q_r + q_i}{1 + q_v}\right)^{-1}. \quad (6)$$

Here, R is the ideal gas constant of dry air, and T_v is the virtual temperature. The thermodynamic equation is given by

$$\frac{\partial p^* T}{\partial t} = -m^2\left[\frac{\partial (p^* T u/m)}{\partial x} + \frac{\partial (p^* T v/m)}{\partial y}\right] - \frac{\partial (p^* T \sigma^\bullet)}{\partial \sigma} + \frac{R T_v \omega}{c_{pm}(\sigma + p_{100}/p^*)} + \frac{p^*[L_c(CD_{vc} - EV_{rv}) + L_s CD_{vi} + L_f(CL_{ci} - ML_{ir})]}{c_{pm}} + DT, \quad (7)$$

where L_c, L_s, and L_f are the latent heat of condensation, sublimation, and freezing, c_{pm} is the specific heat at constant pressure for moist air, D represents the contribution of horizontal and vertical diffusion, and ω is the vertical velocity in p coordinates.

a. Condensation and deposition

Assuming that clouds cannot be supersaturated, the mixing ratios for water vapor q_v, cloud water q_c, and ice q_i, can be determined diagnostically. If water and ice coexist, three cases must be distinguished. At temperatures lower than −35°C no liquid water exists. Note that sensitivity studies with −40°C as the lower boundary for supercooled water show no significant differences in precipitation rates and amounts. In saturated air masses warmer than 0°C only cloud water can exist. In the temperature range between $T_{00} = -35$°C and $T_0 = 0$°C both ice and cloud water coexist. The saturation mixing ratio is defined as the mass-weighted mean of the saturation value with respect to water and ice. Hence, saturation mixing ratios are given as (Lord et al. 1984)

$$q_s = \begin{cases} q_{sw}, & \text{if } q_c \geqslant 0 \text{ and } q_i = 0 \\ q_{si}, & \text{if } q_i > 0 \text{ and } q_c = 0 \\ \dfrac{q_c q_{sw} + q_i q_{si}}{q_c + q_i}, & \text{if } q_c > 0 \text{ and } q_i > 0. \end{cases} \quad (8)$$

Here, q_{si} and q_{sw} are the saturation mixing ratios with respect to ice and water. Whenever the temperature is between −35° and 0°C and the water vapor mixing ratio is higher than the saturation mixing ratio q_s, cloud water and ice crystals are formed. The deposition and condensation is distributed according to Eqs. (9) and (10) with respect to the supercooling of the cloud:

$$\mathrm{CD}_{vc} = (q_v - q_s)\frac{T - T_{00}}{T_0 - T_{00}} r_{vc}\frac{1}{\delta t} \quad (9)$$

$$\mathrm{CD}_{vi} = (q_v - q_s)\frac{T_0 - T}{T_0 - T_{00}} r_{vi}\frac{1}{\delta t}. \quad (10)$$

Herein, δt is the time step (120 s), r_{vc} and r_{vi} stand for $[1 + L_c^2 q_s/(R_v c_p T^2)]^{-1}$ and $[1 + L_s^2 q_s/(R_v c_p T^2)]^{-1}$, respectively. If the air is subsaturated with respect to water and supersaturated with respect to ice, water droplets evaporate and the released water vapor deposits on ice crystals. It is obvious that the terms $(T - T_{00})/(T_0 - T_{00})$ and $(T_0 - T)/(T_0 - T_{00})$ are not necessary when the temperature is lower than −35°C or higher than the freezing point.

Once cloud water is present, rainwater can be built by autoconversion and accretion.

b. Autoconversion

The autoconversion CN_{cr} is taken from Kessler (1969):

$$\mathrm{CN}_{cr} = \begin{cases} \alpha(q_c - q_{c0}), & \text{if } q_c \geqslant q_{c0} \\ 0, & \text{if } q_c < q_{c0}. \end{cases} \quad (11)$$

The onset of autoconversion is controlled by the parameters α and q_{c0}. These parameters are dependent on grid resolution. Values of $\alpha = 10^{-3}\ \mathrm{s}^{-1}$ and $q_{c0} = 0.5\ \mathrm{g\ kg}^{-1}$ are used here, in accordance with Anthes et al. (1987).

c. Accretion

The parameterization of the accretion rate follows Orville and Kopp (1977). Assuming a Marshall–Palmer (1948) distribution for the raindrops and continuous collection, the accretion rate is given by

$$\mathrm{CL}_{cr} = E_r \frac{\pi N_{0r} a \Gamma(3 + b) q_c}{4\lambda_r^{3+b}}, \quad (12)$$

where Γ is the gamma function, and E_r is the collection efficiency of rainwater, which is set equal to 1. The other parameters are chosen as $N_{0r} = 8 \times 10^6\ \mathrm{m}^{-4}$, $a = 842\ \mathrm{m}^{1-b}\ \mathrm{s}^{-1}$, and $b = 0.8$, respectively; λ_r is the size distribution parameter of the raindrops depending on the mixing ratio of rainwater. Also,

$$\lambda_r = \left(\frac{\pi \rho_w N_{0r}}{\rho_a q_r}\right)^{1/4}, \quad (13)$$

where $\rho_w = 10^3\ \mathrm{kg\ m}^{-3}$ and ρ_a are the density of water and air, respectively.

d. Evaporation of rainwater

Rainwater falling through the cloud base will evaporate. The evaporation of raindrops is determined according to Orville and Kopp (1977) by

$$\mathrm{EV}_{rv} = \frac{2\pi(1 - \mathrm{RH})N_{0r}\{0.78\lambda_r^{-2} + 0.32\mathrm{Sc}^{1/3}\Gamma[(b + 5)/2]a^{1/2}\nu^{-1/2}\lambda_r^{-(b+5)/2}\}}{\rho_a\{[L_c^2/(K_a R_v T^2)] + [1/(\rho_a q_{sw} D_v)]\}}, \quad (14)$$

where RH is the relative humidity, ν is the kinematic viscosity of the air, K_a is the thermal conductivity, D_v is the diffusivity for water vapor, R_v is the gas constant for water vapor, and $\mathrm{Sc} = \nu/D_v$ is the Schmidt number. The parameters a, N_{0r}, and λ_r are the same as described in Eqs. (12) and (13).

e. Riming

The ice phase is also a sink for cloud water due to the collection of cloud drops by ice crystals. Cotton et al. (1982) assume that ice-crystal growth processes could be represented by the growth of a mean ice crystal. The mean ice-crystal mass is diagnosed by

$$m_i = \frac{\rho_a q_i}{N_i}, \tag{15}$$

where q_i is prognosed. The ice nucleus concentration N_i is determined by the well-known Fletcher (1962) formula

$$N_i = A \exp[\beta(273.16 - T)], \tag{16}$$

with $A = 10^{-2}$ m^{-3} and $\beta = 0.6$ K^{-1}. Cotton et al. (1982) distinguish between three regimes of ice-crystal growth:

- growth by diffusion on hexagonal plates,
- diffusion and riming on slightly rimed hexagonal plates,
- riming on graupel-like hexagonal particles.

The ice-crystal type is defined by its mass m_i. Diameter and fall velocity of the mean ice particle are given by

$$D_i = k_1 m_i^{1/2} \tag{17}$$

$$u_i = k_2 D_i \left(\frac{\rho_0}{\rho_a}\right)^{1/2} \tag{18}$$

with

$$\left.\begin{aligned} k_1 &= 16.3 \text{ m kg}^{-1/2} \\ k_2 &= 304 \text{ s}^{-1} \end{aligned}\right\} \quad \text{if } m_i < 1.7 \times 10^{-10} \text{ kg} \tag{19}$$

$$\left.\begin{aligned} k_1 &= 6.07 \text{ m kg}^{-1/2} \\ k_2 &= 1250 \text{ s}^{-1} \end{aligned}\right\}$$

$$\text{if } 1.7 \times 10^{-10} \text{ kg} \leqslant m_i < 10^{-8} \text{ kg}. \tag{20}$$

The quantity $(\rho_0/\rho_a)^{1/2}$ is a correction factor to consider the decreasing of the fall velocity with increasing air density; ρ_0 is the density of a standard atmosphere. The diameter D_i and the velocity u_i of graupel-like particles are determined according to Locatelli and Hobbs (1974) by

$$D_i = k_1 m_i^{0.417} \tag{21}$$

$$u_i = k_2 D_i^{1/4} \left(\frac{\rho_0}{\rho_a}\right)^{1/2}. \tag{22}$$

Here, the constants are given by $k_1 = 1.58$ m kg$^{-0.417}$ and $k_2 = 4.84$ m$^{3/4}$ s^{-1}, respectively.

The Fletcher (1962) formula results in too low ice nucleus concentrations at small ranges of supercooling temperatures, which can cause too large ice crystals. In order to avoid this, a lower limit for the nucleus concentration was introduced by

$$N_{i,\min} = \frac{\rho_a q_i}{2.49 \times 10^{-7}}. \tag{23}$$

This value is based on the assumption that the ice crystals may not grow larger than 2.8 mm, which is the uppermost diameter given by Locatelli and Hobbs (1974) for the range in which Eqs. (21) and (22) are valid. Meyers et al. (1992) and Cotton et al. (1986) suggested a modified formulation that corrects the overprediction of ice nuclei in very cold clouds and is sensitive to the saturation conditions. Further research is needed on the problem of the determination of the ice nuclei.

The riming rate due to the collection of cloud drops by ice crystals is calculated by

$$\mathrm{CL}_{ci} = 0.25\pi D_i^2 u_i E_i N_i q_c, \tag{24}$$

where $E_i = 0.8$ is the collection efficiency. Note that tests without the inclusion of riming result in higher cloud water mixing ratios and slightly lower accumulated precipitation amounts.

f. Sedimentation

Cloud droplets are assumed to have no significant fall velocity. Hydrometeors are sufficiently large to have an appreciable fall velocity. Assuming that the spectral density of ice particles is also given by a Marshall–Palmer (1948) distribution (Cotton et al. 1982), the mean mass-weighted terminal velocity for raindrops and ice crystals is calculated by

$$v_{Tr} = \frac{a\Gamma(4 + b)}{6\lambda_r^b}, \tag{25}$$

$$v_{Ti} = \frac{c\Gamma(4 + d)}{6\lambda_i^d}, \tag{26}$$

where $c = 56.4$ m^{1-d} s^{-1} and $d = 0.57$ are constants [a and b as in Eq. (12)]. The size distribution parameter of the ice particles, λ_i, depends on the ice mixing ratio according to

$$\lambda_i = \left(\frac{\pi \rho_i N_{0i}}{\rho_a q_i}\right)^{1/4}, \tag{27}$$

where $N_{0i} = 7.6 \times 10^6$ m^{-4}, and ρ_i is the density of ice. The density of ice depends on the moisture available during the growth process and on the size of the collected drops. Furthermore, the time needed for the freezing of the collected cloud droplet or raindrop is important for the density of the ice (Fletcher 1962). For instance, Locatelli and Hobbs (1974) found values of 20–450 kg m^{-3} for graupel and rimed columns, Zikmunda and Vali (1972) values of 250–700 kg m^{-3} for conical graupel, and Pruppacher and Klett (1980) values of 50–890 kg m^{-3} for snow. As the collection of raindrops is not considered in our study, a value of 84 kg m^{-3} was chosen for the density of ice. Sensitivity studies with ice densities of 600 and 916 kg m^{-3} provided results that hardly differ from those obtained with a value of 84 kg m^{-3}. In the case of higher ice densities the accumulated rain after 72 h of simulation is slightly higher.

TABLE 1. Domain (2880 km × 4880 km) total amounts of cloud water, rainwater, and ice at 1200 UTC 28 April 1986 as simulated by MM4 with the five different MM4 cloud modules and domain total amounts of liquid water and ice rediagnosed by the CTM cloud module for fair weather and raining clouds using the meteorological data of a given MM4 simulation.

	KUO	WARM	KUO + WARM	COLD	KUO + COLD
MM4					
q_v (kg)	2.5×10^{14}	2.6×10^{14}	2.6×10^{14}	2.6×10^{14}	2.5×10^{14}
q_c (kg)	—	2.9×10^{12}	1.7×10^{12}	5.2×10^{11}	3.3×10^{11}
q_r (kg)	—	1.6×10^{11}	9.8×10^{9}	2.1×10^{11}	7.8×10^{10}
q_i (kg)	—	—	—	3.3×10^{11}	2.0×10^{11}
Fair weather clouds					
CTM					
q_l (kg)	1.4×10^{12}	1.7×10^{12}	1.7×10^{12}	1.7×10^{12}	1.6×10^{12}
q_i (kg)	9.7×10^{10}	1.1×10^{11}	1.0×10^{11}	1.1×10^{11}	9.7×10^{10}
Raining clouds					
CTM					
q_l (kg)	6.5×10^{12}	1.3×10^{12}	3.3×10^{12}	4.8×10^{12}	5.5×10^{12}
q_i (kg)	9.8×10^{12}	2.0×10^{12}	5.1×10^{12}	7.8×10^{12}	8.5×10^{12}

g. *Melting*

Ice crystals falling through the freezing level melt and become raindrops. It is assumed that hydrodynamical effects, which are important for small time steps and large crystals, graupel, or hail, can be neglected. The melting rate is given by

$$\mathrm{ML}_{ir} = \frac{q_i}{\delta t}. \tag{28}$$

Note that the melting of the ice crystals generally occurs in the levels below that of freezing due to the resolution of the vertical grid.

3. Outline of the simulations

MM4 was run with the five options mentioned above. A 3-day episode from 25 to 28 April 1986 (the time immediately after the Chernobyl accident) was chosen to study the different cloud parameterizations and their influence on the distribution of atmospheric trace species. The simulation of the episode starts and ends at 1200 UTC of the days mentioned above. The meteorological situation during that time was governed by a cyclone near Iceland and high pressure over northeastern Europe. Over the Alps a low pressure system caused heavy rainfalls [for more details, see Hass et al. (1990)]. Due to these rain events, this episode seems to be of interest for cloud module tests.

The initial data to start the five MM4 simulations are obtained from the NMC (National Meteorological Center). The center of the model was chosen as 50°N, 10°E. A Lambert conformal projection was used. The (x, y, σ) dimensions of the grid are $46 \times 61 \times 15$. The horizontal resolution is 80 km × 80 km. The vertical resolution is nonequidistant; it has eight levels below 2 km for an acceptable representation of the atmospheric boundary layer and seven levels above this height. The top of the model is in $p_{100} = 100$ hPa as mentioned above.

The five predictions of the meteorological fields by MM4 are designated as KUO (cumulus parameterization scheme), WARM (warm scheme), KUO + WARM (warm and cumulus parameterization schemes), KUO + COLD (ice and cumulus parameterization schemes), and COLD (ice parameterization scheme), respectively.

The meteorological data of the five simulations were taken as input data for the cloud and aqueous chemistry module that is usually used in CTM. The chemical initial values were the same for all tests. To avoid changes in concentrations resulting from other than cloud related processes, no complete CTM run is done. Like in EURAD the CTM cloud module is run once per hour to calculate cloud parameters and aqueous-phase chemistry processes for 1-h duration. Therefore, in this study the CTM cloud module is called once at the end of each MM4 run, that is, with the 72d hour of the five meteorological datasets mentioned above because at this time the differences between the results of these MM4 simulations are the largest. The results after 1 h of storm simulation by the CTM cloud module were taken into account to study the influence of the different cloud modules in MM4 on the evolution of the distribution of the gases.

All information on cloud parameters predicted by MM4 except for the rain amount and the water vapor mixing ratio are ignored by the chemistry transport model. The cloud parameters are rediagnosed by the CTM cloud module on the basis of the delivered water vapor data. Since during the MM4 simulations a portion of water has already been removed from the atmosphere as rain, the input data for CTM assume a drier atmosphere. Table 1 shows the amounts of cloud water, rainwater, and ice as well as the liquid water and ice amount rediagnosed by the CTM cloud module

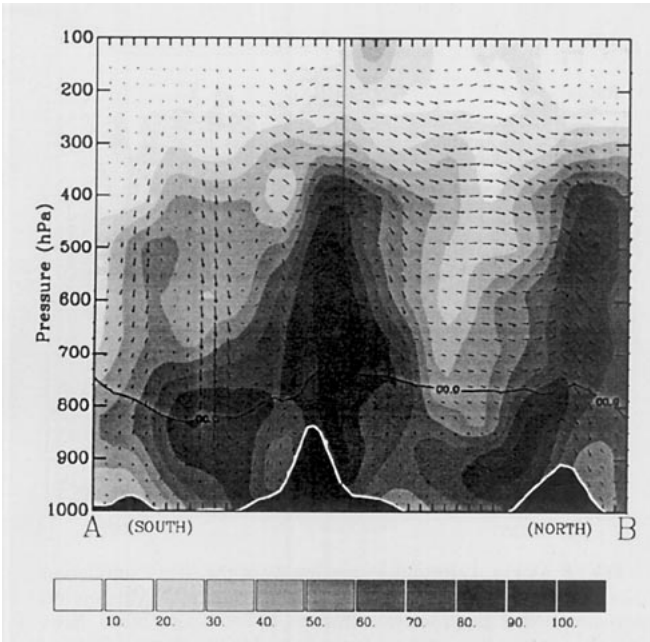

FIG. 1. North–south cross section through the model domain from Tunis in Africa (*A*) to Scandinavia (*B*) and from the surface to the model top (100 hPa). The NMC analysis of 1200 UTC 28 April 1986 are shown. Arrows represent the wind circulation projected into the cross section; relative humidity is displayed by the gray shaded areas. The thick solid line gives the 0°C isotherm. Maximum wind speeds in horizontal and vertical direction are 26.53 m s^{-1} and 0.094 Pa s^{-1}, respectively. The vertical line shows the position of the column discussed in Table 2 and in Figs. 12 and 13.

from this drier atmosphere. As shown here, the values of the total water content rediagnosed by the CTM cloud module are higher than those predicted by the different MM4 cloud modules. The reasons that lead to these awkward results will be discussed later. Note that the KUO simulation does not predict cloud water and/or rainwater at all.

CTM uses an operator splitting technique. At present the CTM cloud module is called by the EURAD model package once per hour, this means that concentration changes due to cloud effects are calculated hourly. During the cloud lifetime aqueous phase chemistry and scavenging processes are calculated at their individual time steps. After each hour of simulation the cloud module loses all information on the polluted state of the cloud water because it is assumed that the cloud totally vanishes after each hour. Thus, all cloud parameters needed for the aqueous-phase chemistry calculations are recalculated by the CTM cloud module from hourly MM4 data, and the aqueous-phase concentrations are determined using the gas-phase concentrations and the relevant cloud parameters.

We must assume that the different meteorological datasets result in different values of cloud parameters in CTM. Furthermore, we must accept that the inconsistencies in the architecture of the EURAD model package mentioned in the Introduction can influence the chemical processes and, hence, can lead to different amounts of wet deposition rates. In order to get a clearer view of the effects of the treatment of cloud physics in MM4 on the results of the cloud module used in CTM, the whole model domain is initialized with the same vertical profiles of pollutants. This form of initialization suppresses horizontal concentration gradients due to transport, emissions, etc. The initial profiles used here represent a polluted atmosphere like in the leeside region of industrial areas and urban conurbations. The rediagnosed cloud parameters are compared with each other and with those of the MM4 simulations, and the results of cloud chemistry simulation after 1 h of simulation are compared with each other, as well. The CTM simulations are denoted as KUO, WARM, COLD, KUO + WARM, and KUO + COLD, respectively, according to the MM4 data used as input data for the CTM cloud module.

4. Results of MM4 predictions

In this section the results of the different MM4 predictions are compared and discussed. The focus will be on the parameters that are important for the cloud chemistry module, such as water vapor mixing ratio, rain amount, and temperature.

a. Pressure, wind circulation, and temperature

Generally, the wind fields show their largest differences with respect to the analysis in the regions of the cloud systems for all simulations. They differ significantly from that of the analysis especially over the Mediterranean Sea (Figs. 1–6). The wind circulation predicted by the COLD simulation agrees the best with that of the analysis, but even this prediction is not satisfying. In comparison with the satellite data, all five simulations produce a temporal offset of about 2 h in the location of the predicted cloud systems, that is, the positions of the cloud fields predicted for the time 2 h after the satellite passage match best with the positions observed from the satellite during its passage. The reasons for this temporal offset may be found in the neglect of further subscale and microphysical processes.

In comparison with each other, the simulations using the warm scheme (WARM, KUO + WARM) do not provide significant differences in the temperature and wind fields. The same is true for the simulations with ice parameterization (COLD, KUO + COLD), where, however, the differences are a little bit larger. The COLD simulation calculates slightly lower temperature values than the WARM simulation, where the discrepancies result from the different amounts of the released latent heat or absorbed heat. In the cloudy regions the KUO simulation predicts up to 3-K-higher temperatures than do the other simulations.

b. Cloud parameters

Figure 1 shows the analysis of the relative humidity and wind circulation on 1200 UTC 28 April 1986.

Areas of high relative humidity are found over the Alps and Scandinavia reaching up to the 300-hPa level. The corresponding results of the simulations with the five different MM4 options are presented in Figs. 2–6. In all simulations the predicted relative humidity is too high in comparison with the analysis. In the upper model layers the values of relative humidity predicted by the WARM simulation are higher than those provided by the other runs. Consequently, the cloud tops reach higher levels (Fig. 3). As shown in Figs. 3 and 4, not only the vertical, but also the horizontal extension of the clouds is larger for the simulation using the warm scheme (WARM, Fig. 3; KUO + WARM, Fig. 4).

The reason for these warm-scheme phenomena is that a lot of moisture is lifted into higher levels due to strong vertical motions at the French Riviera. Once built in the upper levels, the cloud water is transported northeastward. Since the cloud water mixing ratio is not beyond the threshold value used by the Kessler parameterization for the onset of rainwater formation, no rain is formed. Thus, evaporation until saturation is reached is the only sink for cloud water. Consequently, the upper model domain is moistened during the transport of cloud water. In contrast, clouds containing ice also lose water by sedimentation. Hence, the cloud tops are found in lower levels than those predicted without ice parameterization (Figs. 3–6). Since the ice content and the terminal velocity are much lower in the KUO + COLD simulation than in the COLD run (because the cumulus parameterization scheme is also able to remove water vapor), the cloud tops are reaching higher in the case of the KUO + COLD run than in the latter case (Figs. 5 and 6). Note that at some grid points only one of the simulations predicts clouds. This is due to the differences in the distributions of relative humidity caused by different dynamics and microphysical processes.

The WARM and COLD simulations, of course, predict similar distributions of cloud water mixing ratios (± 0.05 g kg^{-1}) when the temperature is above freezing. But in the upper model domain (at temperatures below 0°C) large differences exist. Since the ice crystals grow at the cost of cloud droplets and precipitation is also formed via the ice phase, the maxima of cloud water mixing ratios predicted by the WARM simulation occur in higher levels (Figs. 3 and 5).

In some clouds of the COLD and/or KUO + COLD simulations rainwater is formed only via the ice phase (Figs. 5 and 6). Therefore, no rainwater occurs at these grid points for the simulations without ice parameterization (WARM, KUO + WARM; Figs. 3 and 4).

Since the cumulus parameterization scheme does not predict any liquid or solid cloud particles, in the case of the KUO simulation only the relative humidity is presented (Fig. 2). The cumulus parameterization scheme allows the development of clouds only if the horizontal moisture convergence exceeds a critical

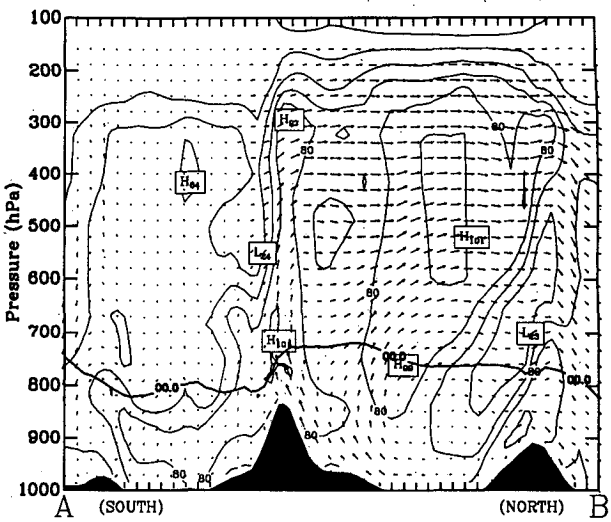

FIG. 2. As Fig. 1. Results shown are from the MM4 simulation using the cumulus parameterization scheme (KUO). This option does not predict cloud water, rainwater, or ice mixing ratios. Note that the contour lines of the relative humidity are given in 20% intervals. Maximum wind speeds in horizontal and vertical direction are 25.21 m s^{-1} and 0.080 Pa s^{-1}, respectively.

value. Thus, the areas where clouds occur are restricted in comparison with the other runs where only supersaturation is required. The atmosphere predicted by the KUO simulation is drier than those predicted by the other simulations because all condensate is treated to fall out immediately, that is, within one time step. Furthermore, the excess moisture that has not been removed by the cumulus parameterization is also treated to be precipitated immediately if the air is supersaturated. No evaporation below the cloud is included. In contrast to this, the warm scheme and ice parameterization condense or deposit all excess moisture, but the predicted hydrometeors do not inevitably reach the ground. Furthermore, as already mentioned, these schemes also allow the raindrops and/or ice crystals to evaporate in subsaturated layers. Consequently, these layers may be moistened and, hence, the relative humidity may increase.

c. *Precipitation*

The pattern of the observed precipitation has already been presented by Hass et al. (1990). This pattern was derived from land-based measurements that, however, were performed only from 0600 UTC 26 April 1986 to the end of the episode. In view of these facts, the pattern of the observed precipitation is not shown here. In the further discussion of the predicted precipitation only the forecasts over land are compared with the observations.

The rain rate determined by the KUO simulation is too high in comparison with the observed precipitation data (Fig. 7). In nature, nonprecipitating

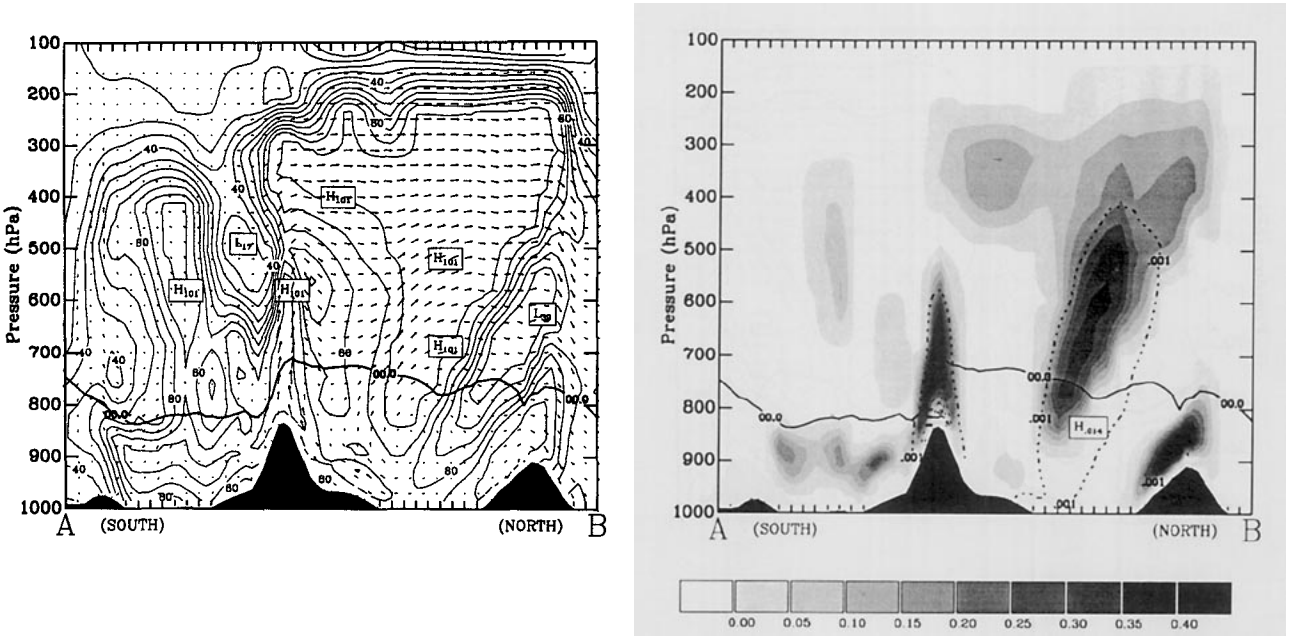

FIG. 3. (a) As Fig. 1 but for the MM4 simulation using the warm scheme (WARM). (b) Mixing ratios (g kg^{-1}) for the cloud water (filled areas) and rainwater (dashed lines). The contour intervals are from 0.001 to 0.45 g kg^{-1} by 0.05. The thick solid line gives the 0°C isotherm. This option does not predict ice. Note that the contour lines of the relative humidity are given in 10% intervals. Maximum wind speeds in horizontal and vertical direction are 25.35 m s^{-1} and 0.105 Pa s^{-1}, respectively.

cumulus clouds were probably formed while raining clouds were predicted. The horizontal patterns (Fig. 8) are larger than those of the other simulations shown for the main simulations WARM and COLD in Figs. 9 and 10. The reason is that of the total horizontal water vapor convergence in a column a fraction is condensed and precipitated out of the column. The remaining fraction is stored and increases the humidity of the column. Contrary to the cumulus parameterization scheme, the clouds that

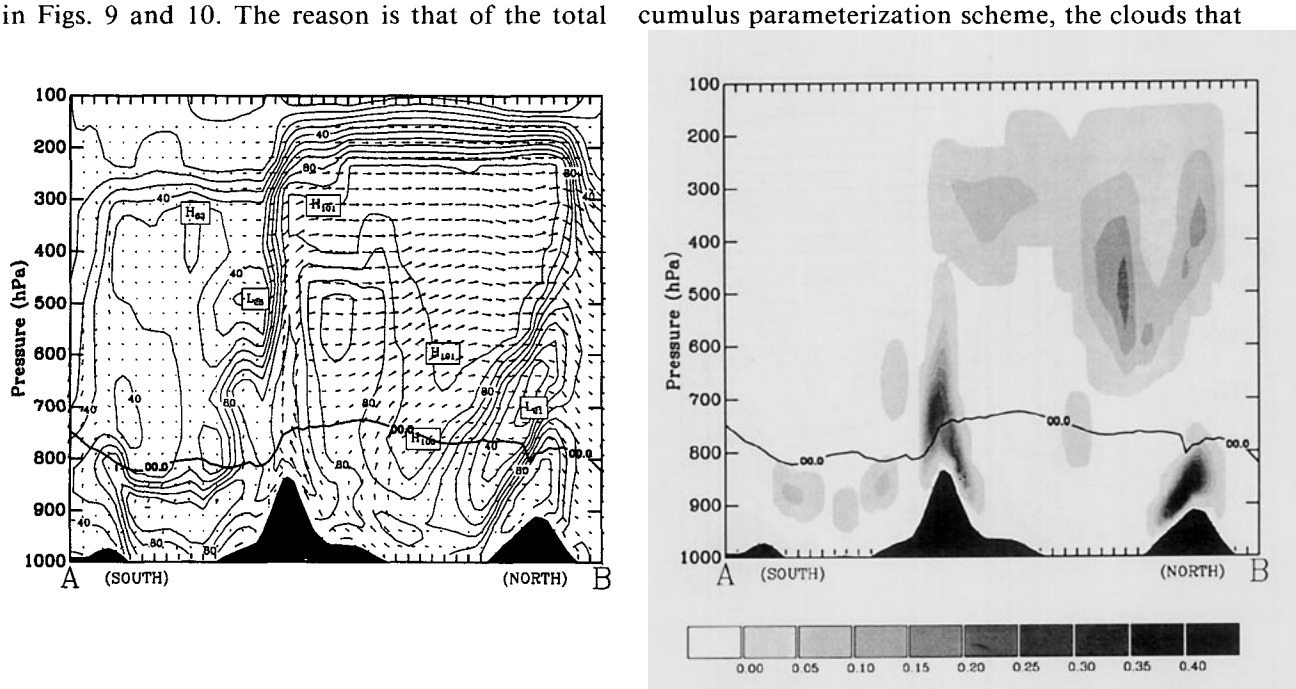

FIG. 4. As Fig. 3 but for the MM4 simulation using the warm scheme and the cumulus parameterization (KUO + WARM) concurrently. Note that rainwater occurred only north of the Alps (values are less than 0.0025 g kg^{-1}). This option does not predict ice. Note that the contour lines of relative humidity are given in 10% intervals. Maximum wind speeds in horizontal and vertical direction are 24.95 m s^{-1} and 0.078 Pa s^{-1}, respectively.

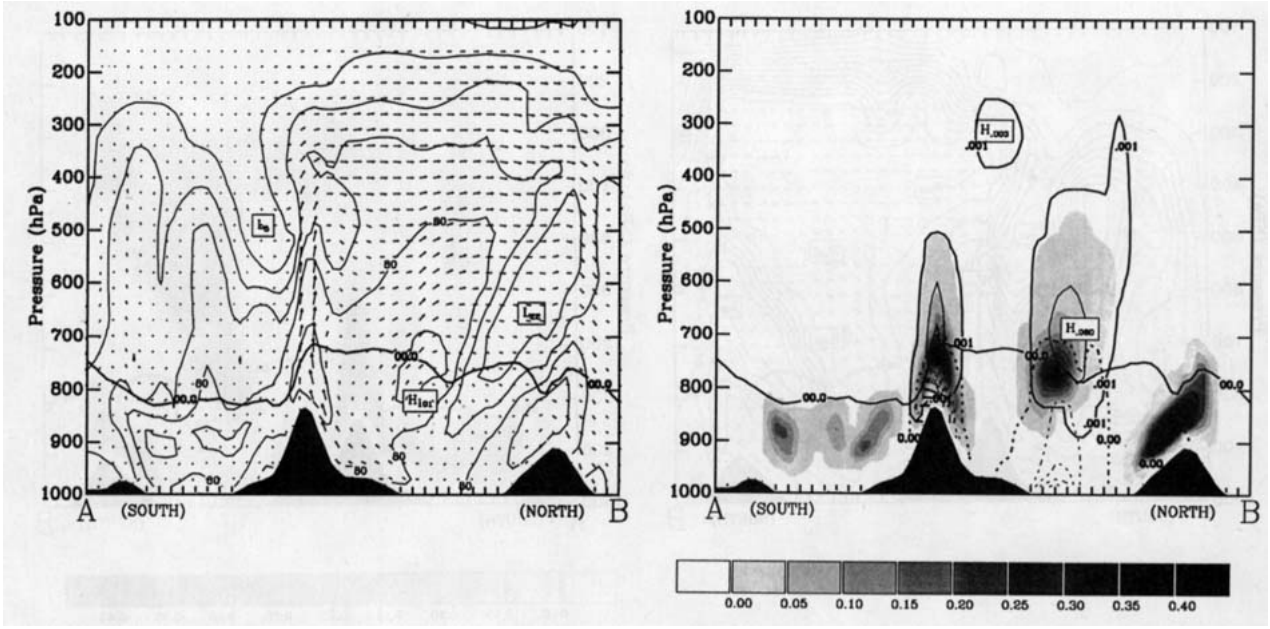

FIG. 5. (a) As in Fig. 3 but for the MM4 simulation using the ice parameterization (COLD). (b) Mixing ratios (g kg^{-1}) for the cloud water (filled areas), rainwater (dashed lines), and ice (solid lines). The contour intervals are from 0.001 to 1 g kg^{-1} by 0.05 and from 0.001 to 0.1 g kg^{-1} by 0.05 for rainwater and ice, respectively. Note that the contour lines of the relative humidity are given in 20% intervals. Maximum wind speeds in horizontal and vertical direction are 26.35 m s^{-1} and 0.121 Pa s^{-1}, respectively.

are formed by the other parameterization schemes do not necessarily precipitate.

The precipitation fields predicted by the WARM simulation (Fig. 9) show less horizontal gradients and less horizontal extension than those predicted by the other runs. Furthermore, the WARM simulation strongly underestimates the rainfall rates during the first 36 h and performs better afterward (Fig. 7). Since satellite data evidence high amounts of ice clouds during the simulated episode, a possible reason for this

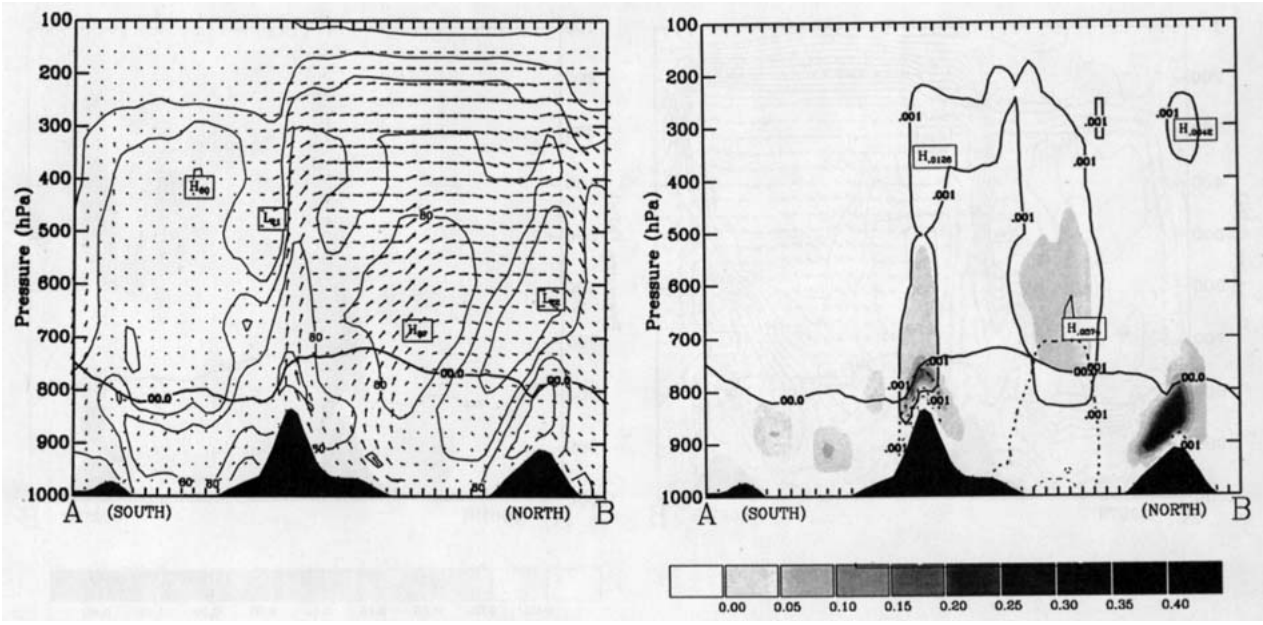

FIG. 6. As in Fig. 5 but for the MM4 simulation using the cumulus and the ice parameterization (KUO + COLD) concurrently. The contour intervals are from 0.001 to 0.15 g kg^{-1} by 0.05 and from 0.001 to 0.05 g kg^{-1} by 0.05 for rainwater and ice, respectively. Note that the contour lines of the relative humidity are given in 20% intervals. Maximum wind speeds in horizontal and vertical direction are 26.08 m s^{-1} and 0.080 Pa s^{-1}, respectively.

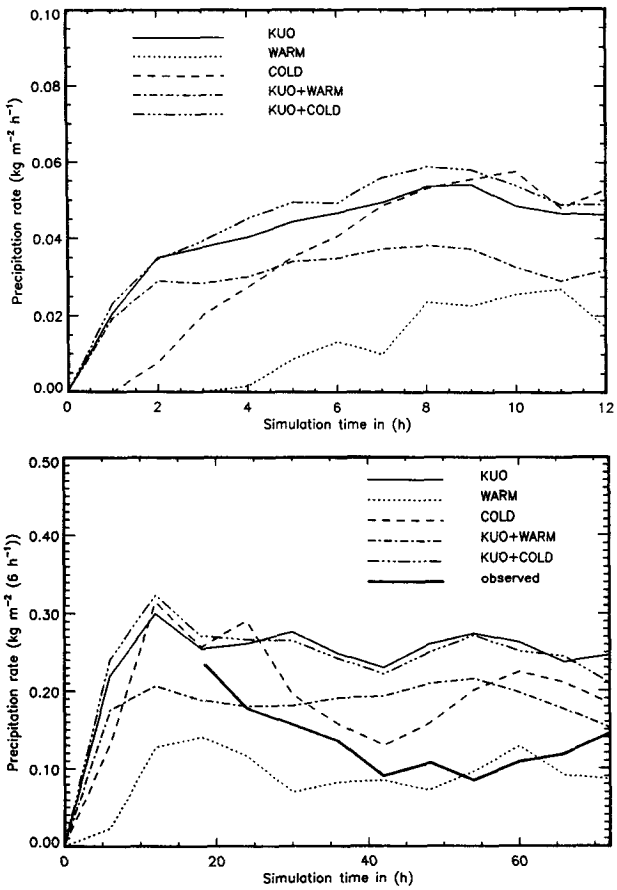

FIG. 7. Domain-integrated rain rate for the MM4 simulations. The upper figure shows the domain integrated precipitation rate of the first 12 h of the simulations for every hour. The lower figure shows the domain integrated precipitation rate every 6 h for the complete 72 h of the simulations. The thick solid curve represents the rain data as observed over land in the model domain (25°–60°N, 10°W–40°E). Note that no data were available before 0600 UTC 26 April 1986.

underestimation is that the precipitation was also formed via ice-phase processes during that episode. Taking threat score, bias score, and categorical score into account, the rain forecasts of the COLD simulation (Fig. 10) agree best in most cases with the observed precipitation data. The inclusion of ice microphysics (COLD) also has the effect that precipitation is initiated earlier (which also is an important point for wet deposition) than in the WARM simulation (Fig. 7). First of all, the saturation mixing ratio of ice is lower than that of water. Furthermore, in the precipitation formation via the ice phase no threshold value (like in the Kessler parameterization of the warm scheme) must be exceeded before sedimentation begins. The presence of ice is decisive.

The precipitation rates for the combined runs (KUO + WARM, KUO + COLD) are higher than those for WARM and COLD (Fig. 7). The onset of precipitation

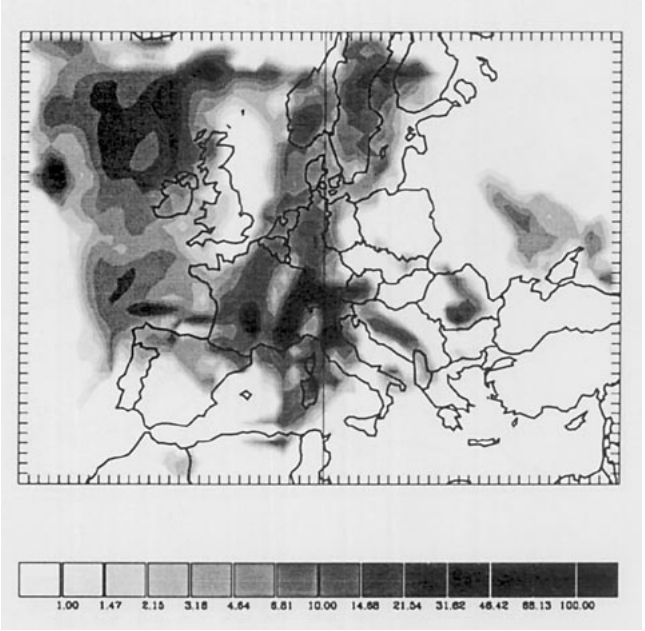

FIG. 8. The 72-h accumulated total rain (mm) as calculated by the MM4 run using the cumulus parameterization scheme (KUO). The horizontal line marks the cross sections considered in Figs. 1–6.

in the combined simulations is earlier than that of the COLD run and the WARM simulation because the included cumulus parameterization allows precipitation just from the beginning of the simulation when the horizontal moisture convergence is large enough. Since in nature convective, ice, and stratiform clouds occur together, the KUO + COLD should perform at

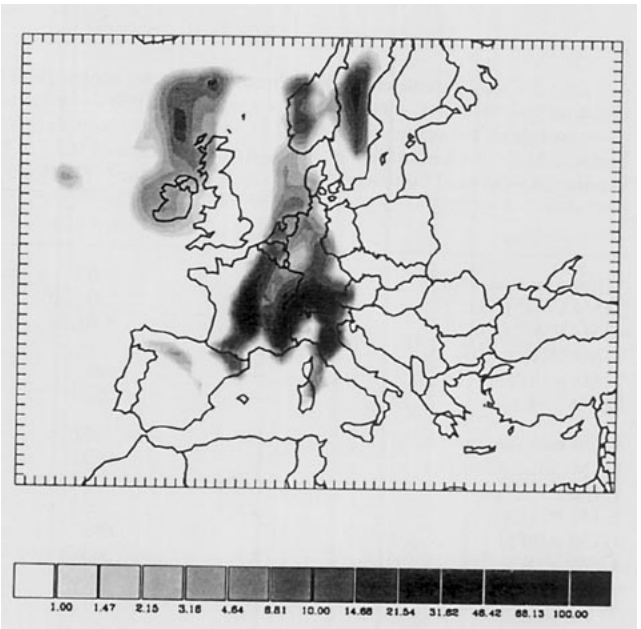

FIG. 9. The 72-h accumulated total rain (mm) as calculated by the MM4 run using the warm scheme (WARM).

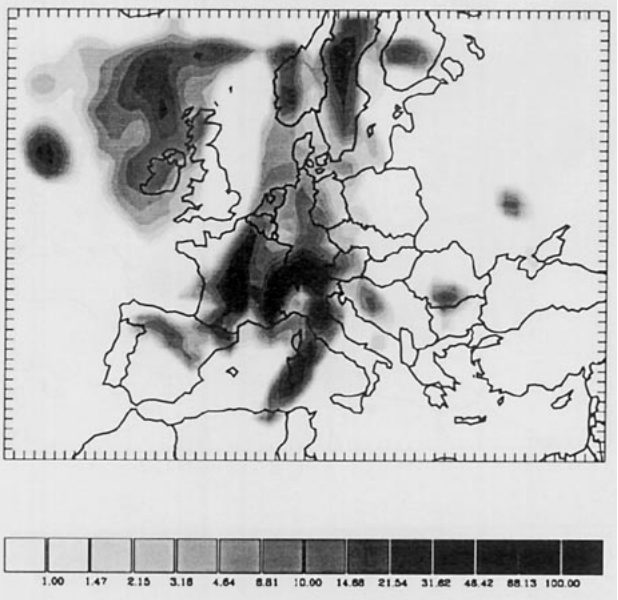

FIG. 10. The 72-h accumulated total rain (mm) as calculated by the MM4 run using the ice parameterization (COLD).

best. This is false because the two parameterization schemes compete for the available moisture.

On the one hand the cumulus parameterization scheme cannot provide cloud water, rainwater, and ice (if included) by itself; on the other hand, it cannot consider the cloud water, rainwater, and ice predicted by the warm scheme or ice parameterization scheme, either. These problems and the results obtained by the combined simulations illustrate that these modules should not be used together without modifying the cumulus parameterization scheme with respect to the treatment of condensate and precipitation.

Although strong convection occurred during the simulated episode and the COLD simulation was performed for a horizontal resolution that is more appropriate for the KUO run, in our case studies the ice parameterization provided the best forecast for the precipitation and moisture fields with respect to the estimation skills.

5. Effects on the simulation results of the CTM cloud module

In this section the impacts of the different MM4 cloud modules on the results of the stand-alone version of the CTM cloud and scavenging module are illustrated on the example of a 1-h simulation of the CTM cloud module using the meteorological data provided by the five different MM4 runs after 72 h of simulation. Specifically, the differences in cloud parameters such as cloud cover, mean cloud temperature, mean cloud pressure, and mean liquid water content are investigated. As an example the cloud parameters predicted by MM4 for the column marked in Fig. 1 and the corresponding cloud parameters diagnosed by the CTM cloud module are given in Table 2.

a. Cloud cover

The rain amount and distribution predicted by MM4 are attached to the occurrence and cloud cover of raining clouds. This cloud cover is determined according to Chang et al. (1987) by

TABLE 2. Cloud parameters (LWC—mean liquid water content) and rain rate determined by the CTM cloud module and the corresponding cloud parameters (CWC—mean cloud water content, RWC—mean rainwater content, IC—mean ice content, p—mean pressure in cloud, T—mean cloud temperature) predicted by MM4 for the exemplary cloud shown in Fig. 12. The wet deposition (WD) determined by CTM is given. MM4 does not calculate cloud cover. The data of the 72d hour KUO, WARM, KUO + WARM, COLD, and KUO + COLD simulation were used as meteorological input data to the CTM cloud module.

	KUO	WARM	KUO + WARM	COLD	KUO + COLD
MM4 rain rate (mm h^{-1})	0.7	0.9	0.6	1.4	1.3
MM4 CWC (g m^{-3})	—	0.330	0.101	0.057	0.024
MM4 RWC (g m^{-3})	—	0.054	0.001	0.043	0.003
MM4 IC (g m^{-3})	—	—	—	0.063	0.025
MM4 p (hPa)	—	698	702	828	822
MM4 T (K)	—	262.1	261.2	270.9	269.4
CTM rain rate (mm h^{-1})	2.2	0.6	2.2	0.3	2.3
CTM cloud cover (%)	33	100	29	100	53
CTM LWC (g m^{-3})	0.421	0.135	0.469	0.187	0.481
CTM IC (g m^{-3})	0.378	0.476	0.396	0.226	0.396
CTM p (hPa)	803	682	812	688	815
CTM T (K)	272.1	263.2	272.2	263.5	272.3
pH	3.7	3.7	3.7	3.7	3.7
WD $SO_4^=$ (mg ha^{-1})	4.3	1.4	3.7	1.5	6.9
WD NH_4^+ (mg ha^{-1})	0.66	0.42	0.54	0.41	1.06
WD NO_3^- (10^{-3} mg ha^{-1})	2.1	1.2	1.7	1.0	3.4

TABLE 3. Percentage of the model boxes where raining and fair weather clouds occur for the different simulations.

Simulation	Raining clouds	Fair weather clouds	Total
KUO	18.3	19.6	37.6
WARM	3.4	21.9	25.3
KUO + WARM	9.0	23.3	32.3
COLD	9.8	21.6	31.4
KUO + COLD	11.4	23.2	34.6

$$B = \frac{\tau_c}{\epsilon} \frac{\mathrm{RR}_{\mathrm{MM4}}}{Q_{xs}}, \tag{29}$$

where τ_c is the lifetime of the cloud, Q_{xs} is the rain rate determined by the CTM cloud module, in accordance with Eqs. (23)–(30) of Chang et al. (1987), $\epsilon = 0.3$ is the storm efficiency, and $\mathrm{RR}_{\mathrm{MM4}}$ is the precipitation rate predicted by MM4. In CTM the cloud cover of fair weather clouds depends only on the relative humidity at cloud base, which is defined as the lifting condensation level (Hass et al. 1993). Their occurrence is restricted in CTM because fair weather clouds higher than the 650-hPa level are rejected. Table 3 represents at how many grid points raining or fair weather clouds occur for the experiments started with the outputs of the five different MM4 runs. Since MM4 does not predict the cloud cover, only that determined by CTM is discussed. Due to the parameterization of a vertically integrated cloud cover of a representative cloud as used in CTM, discrepancies between the observed and the predicted cloud cover can occur; for example, if two atmospheric layers each contained a cloud of 10% cloud cover and do not overlap, the satellite would see 20%, while the cloud module would (correctly) predict 10% for both layers. Furthermore the often observed overlapping of clouds in different atmospheric layers cannot be considered in the model. Note that from satellite, for instance, low-level clouds under high-level clouds cannot be detected.

Generally, too little clouds are diagnosed for all simulations. There are only a few clouds in the WARM simulation of MM4 (Table 3) because its predicted rain rate is lower than that of all other runs and the atmosphere is more humid so that a higher rain rate can be predicted by the CTM cloud module, which leads to a smaller cloud cover [see Eq. (29)]. The amount of fair weather clouds is also low because of the restriction in the cloud height mentioned above. Figure 11 shows the cloud cover at 1325 UTC 27 April 1986 determined from *NOAA-9* satellite data and that derived from the KUO simulation. The cloud cover diagnosed by the CTM cloud module with the data of the KUO simulation agrees at best with the clouds detected from the satellite because the cloud cover parameterization [Eq. (29)] was developed for this model configuration. Since the "best" diagnosed cloud cover is already poor, the presentation of the others is renounced. Considering not only the cloud cover, but also the cloud distribution, it is found that for all simulations except for the KUO run the cloud occurrence is lower when diagnosed by the CTM cloud module than that prognosed by the different MM4 cloud modules. This inconsistency is attributed to the fact that the cumulus parameterization used in CTM is more restrictive to allow the occurrence of a cloud than the warm scheme or the ice parameterization scheme, which only demand supersaturation. Furthermore, as already mentioned in the Introduction, the CTM cloud module ignores the ice, cloud water, and rainwater

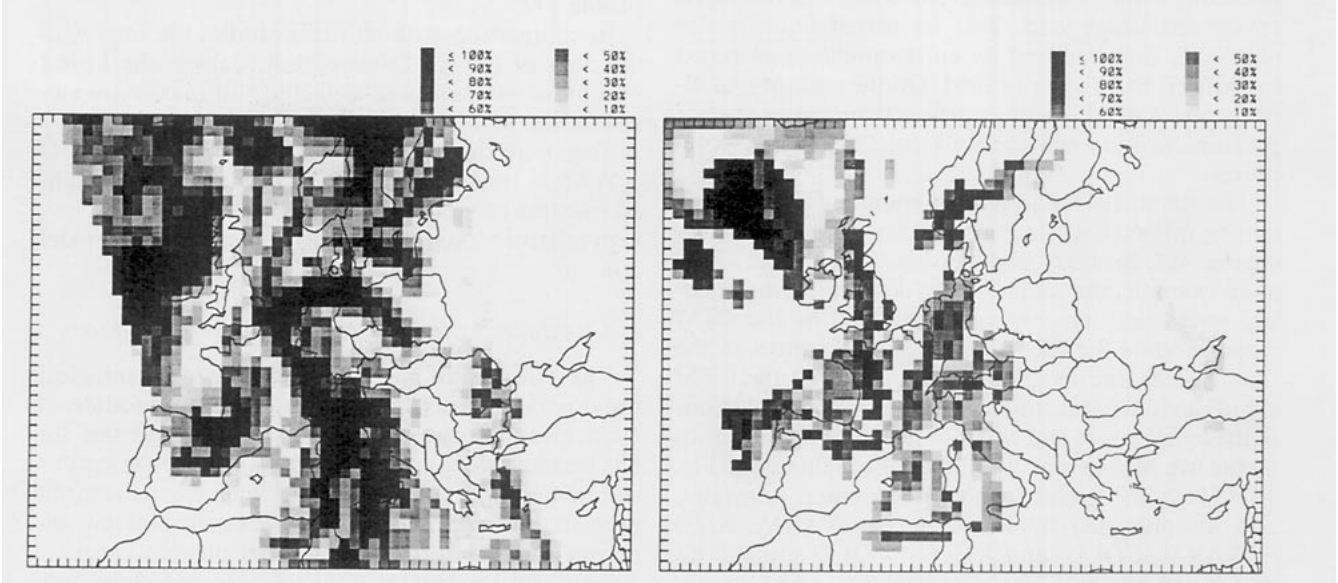

FIG. 11. (a) shows the cloud cover for 1325 UTC 27 April 1986. The free areas at the sides of the model domain are not seen by the *NOAA-9* satellite in this passage. (b) The cloud distribution as predicted by the CTM cloud module with the KUO simulation as input. Note that the *NOAA-9* satellite data were only available for the case shown here.

predicted by MM4. Remember that the ice parameterization performed the best forecast of the horizontal cloud distribution. The discrepancy between this prognosed cloud distribution and the corresponding rediagnosed cloud distribution raises the demands for a consistent treatment of the clouds within EURAD and for a new cloud parameterization scheme. Since the KUO + COLD simulation describes both stratiform and cumuliform clouds, its results should perform the best. This is false because of the reasons discussed above.

Table 2 lists, among others, the cloud cover predicted by the five experiments for the column marked in Fig. 1. The different cloud distributions and cloud covers alter the wet chemistry as well as wet and dry deposition. The photolysis rates are modified according to cloud amount and vertical extension (Chang et al. 1987). Thus, the gas-phase chemistry is also influenced due to differences in cloud cover. Note that the wet deposition depends on the vertical integrated mean rain rate in the cloud domain, on the mean concentration in aqueous solution, and on the cloud cover.

b. Water content and precipitation

In most cases the liquid water content computed by the CTM cloud module for a grid column is higher than that prognosed by the MM4 simulations WARM, KUO + WARM, COLD, and KUO + COLD for the same column. Tests showed that the liquid water content diagnosed by CTM can be up to ten times higher than those prognosed by the MM4 cloud modules. This is due to the different parameterization of the water content. In the CTM cloud module the liquid water content is determined by a parcel of air that rises adiabatically from cloud base to cloud top and retains its condensed water load. The calculated liquid water content is then reduced by entrainment as proposed by Walcek and Taylor (1986). On the contrary, as already mentioned, in the warm scheme or in the ice parameterization scheme only supersaturation is required.

The amount of liquid water content in CTM defines, among others, the relative efficiency of in-cloud scavenging, wet chemistry, and wet deposition. Table 2 lists, as an example, the rain rate, wet deposition, mean liquid water, and ice content determined by the CTM cloud module for the five studies. Differences in the liquid water and ice content diagnosed by the CTM cloud module result from differences in the predictions of the temperature and of the water vapor mixing ratios by the five MM4 simulations (see also Table 2 and Fig. 12). Here, the neglect of the cloud water, rainwater, and ice predicted by MM4 in the WARM, KUO + WARM, COLD, and KUO + COLD simulations performed by the CTM cloud module plays an important role. The model domain–integrated liquid water is the lowest for the tests carried out with the MM4

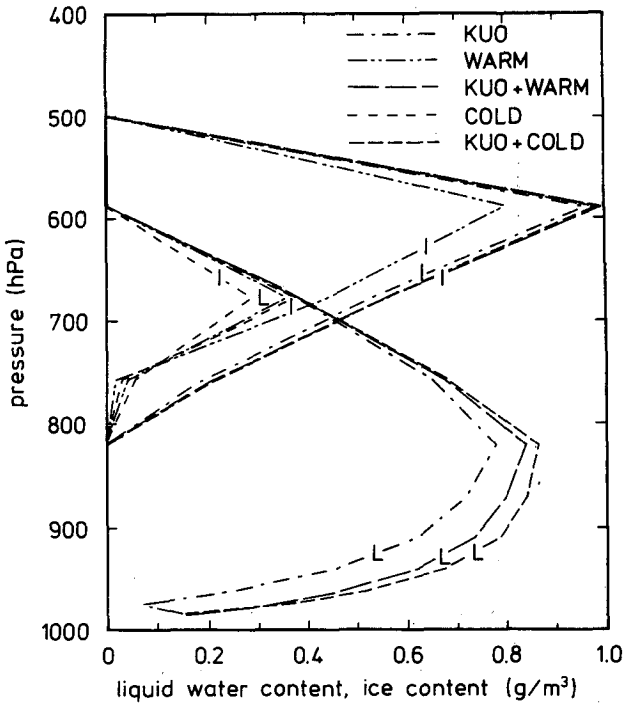

FIG. 12. Impact of five MM4 cloud modules on the determination of the liquid water and ice content by the CTM cloud module for the column marked in Fig. 1 at 1200 UTC 28 April 1986. The data of the MM4 simulations with the cumulus parameterization (KUO), the warm scheme (WARM), the warm scheme plus cumulus parameterization (KUO + WARM), the ice parameterization (COLD), and the ice plus cumulus parameterization (KUO + COLD) are used as start values for the CTM cloud module.

data of the WARM simulation and the highest for those of the KUO and KUO + COLD simulations (Table 1).

In comparison with all other studies the tests with the data of the KUO simulation deliver the lowest minimum values as well as the highest maximum values for the liquid water content.

Tests with the MM4 data of the WARM and KUO + WARM runs as input data usually provide the highest maxima of ice content in CTM because of the very high relative humidity in the upper levels of the model domain.

c. Cloud mean pressure, cloud base, and cloud top

The cloud mean pressure is another meteorological input parameter to the aqueous chemistry module. It is the mean pressure from cloud top to cloud base for fair weather clouds and from cloud top to the earth's surface for raining clouds. Large differences in the mean pressures of the clouds occur between the different experiments because the cloud mean pressure strongly depends on the heights of cloud base and cloud top, which vary between the simulations and were caused by differences in the predictions of the temperature

and moisture fields. Sometimes the difference in the cloud-top height is only a few meters. However, the low vertical resolution of 1–3 km in the upper part of the model can simulate large differences in the cloud tops and thus in the mean cloud pressure. In Fig. 12 the differences in the predicted cloud extensions are shown for the example illustrated in Table 2. Note that differences in the mesoscale pressure fields predicted by the five MM4 simulations show no significant effects on the cloud mean pressure.

Furthermore, large differences occur between the cloud extension obtained by MM4 and that rediagnosed by CTM. These unnecessary inconsistencies in the predicted cloud extensions between MM4 and CTM limit the confidence in the predicted concentration distributions and in the calculated wet deposition. The vertical cloud extensions, for instance, are the highest for the WARM simulation (Fig. 3), but the cloud extensions rediagnosed by the CTM cloud module from these WARM data are usually smaller than those of all other experiments. The tests based on the combined MM4 simulations (KUO + WARM, KUO + COLD) show lower cloud bases than those based only on the individual MM4 cloud parameterization schemes. The mean cloud tops determined with the data of the KUO + WARM run as input to the CTM cloud module usually reach higher than those of the other inputs.

Note that the wet chemistry, wet removal, and vertical mixing due to entrainment as well as the mean concentration of the gases in the cloud depend on the cloud extension (see also Figs. 12 and 13). Furthermore, the height of the cloud base plays a significant role because the gas-phase concentrations are changed in the levels below the cloud base due to decreased photolysis rates and/or washout effects.

d. Mean cloud temperature

The fourth meteorological parameter used in the aqueous chemistry module is the mean cloud temperature. This temperature varies about 3 K between the five studies. The reasons for this fact are differences in the temperatures of the predicted meteorological input data and the already discussed differences in the cloud extension diagnosed by the CTM cloud module. Similar to the liquid water content the mean cloud temperature shows lower minimum as well as higher maximum values for the KUO simulation than for all other runs. The mean cloud temperatures used in the example for the wet chemistry simulations discussed below are given in Table 2. The differences between the mean cloud temperature in MM4 and that diagnosed by the CTM cloud module sometimes exceed more than 10 K (see, e.g., Table 2).

e. pH value

The solubility and transformation of soluble and reactive gases are functions of the pH value. The pH values obtained from the different simulations for the example shown in Fig. 12 are listed in Table 2. There are only slight differences in the predicted pH values.

The KUO simulation diagnoses the highest as well as the lowest pH values because the KUO simulation predicts the highest as well as the lowest mean liquid water content and cloud mean temperatures.

f. Cloud chemistry

The wet removal of trace species depends on their solubility and on their chemical reactions in water. In the CTM cloud module three classes of chemical compounds are considered: The first class contains the soluble gases without chemical production or destruction (e.g., NH_4, HNO_3), which are only vertically redistributed by entrainment and scavenged by drops; the second class lodges soluble gases that react with other tracers (e.g., SO_2, $SO_4^=$, H_2O_2), and the third class contains insoluble nonreactive passive tracers. Note that the species of the latter case are not discussed here because no transport effects, with the exception of entrainment, are taken into account. The entrainment, of course, is different for the five experiments as differences exist in water content, cloud location, and cloud extensions. The highest maximum values for the concentrations of $SO_4^=$ in aqueous solution are found in the results of the KUO simulation. The maximum values are predicted at different locations by the five simulations. The simulations with the WARM and COLD data as input data for the CTM cloud module show similar $SO_4^=$ distributions if clouds occur in both simulations.

A comparison of the CTM cloud module experiments using data of MM4 simulations with the cumulus parameterization (KUO, KUO + WARM, KUO + COLD) with each other shows an increasing spread of HSO_3^-, $SO_4^=$, NO_3^-, and SO_2 in aqueous solution with increasing solution. The comparison of the results of the KUO run with those of the COLD simulation evidences this increase only for the solved NO_3^- and $SO_4^=$. The maxima of soluble HSO_3^- are at quite different locations for the different studies even if their values are of the same order of magnitude. The HSO_3^- concentration in aqueous solution is the lowest for the WARM simulation, and highest for the KUO + WARM simulation, but the concentration fields are more differentiated in the cases of COLD and KUO + COLD.

At most grid points the concentrations of SO_2 in air are higher for the data of the KUO run than for those of the WARM and COLD simulation. Here, the amount of liquid water content is important. The study with the data of the WARM simulation as input provides about 2-ppb-lower concentrations than all other simulations. The SO_4 concentrations vary little between the simulations using the data obtained by the COLD and KUO + COLD simulations. The SO_4 distribution

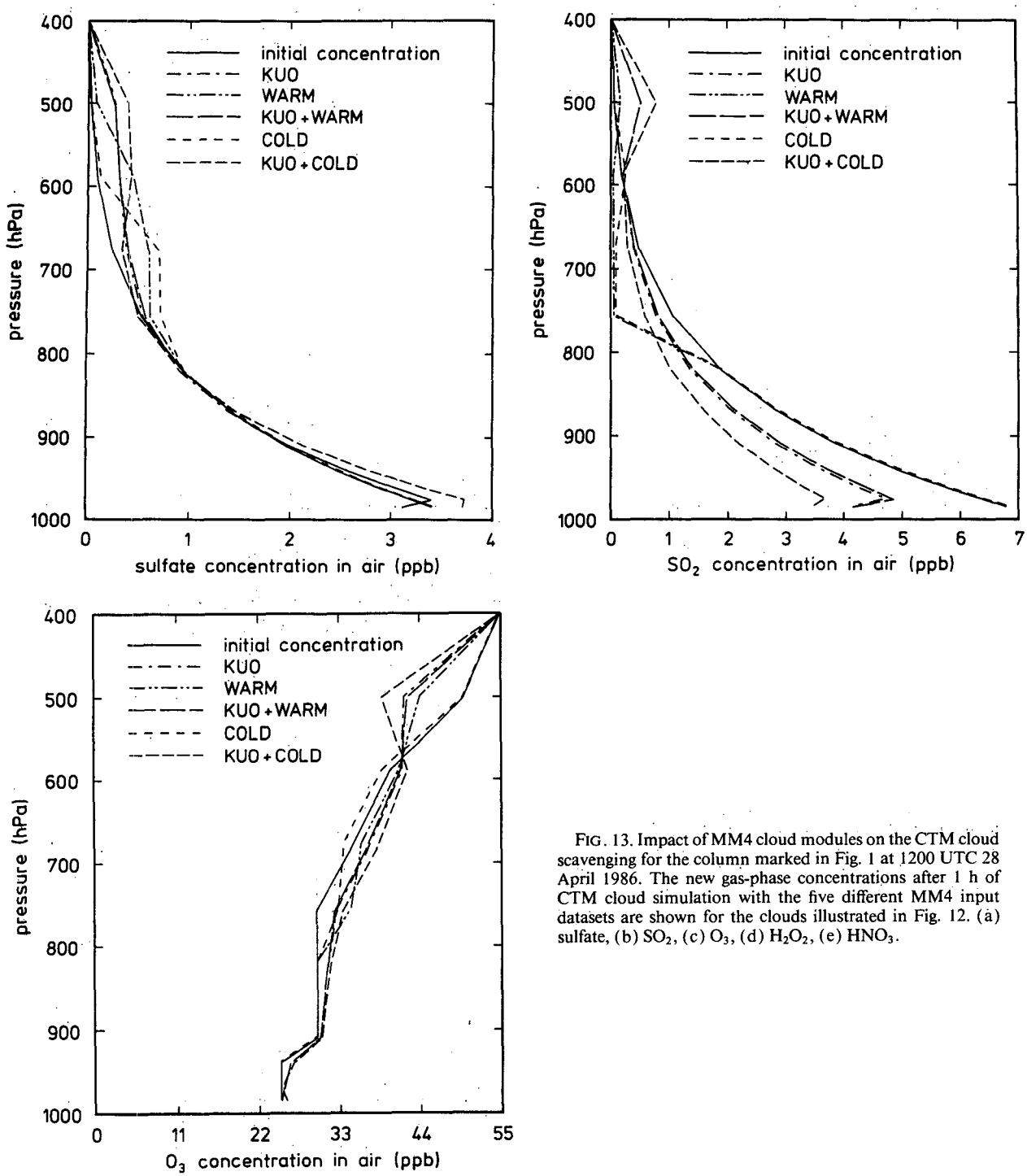

FIG. 13. Impact of MM4 cloud modules on the CTM cloud scavenging for the column marked in Fig. 1 at 1200 UTC 28 April 1986. The new gas-phase concentrations after 1 h of CTM cloud simulation with the five different MM4 input datasets are shown for the clouds illustrated in Fig. 12. (a) sulfate, (b) SO_2, (c) O_3, (d) H_2O_2, (e) HNO_3.

is similar for the data of the WARM and COLD simulations if clouds occur in both simulations. The areas of high concentrations of NO_2 show the largest horizontal extension for the KUO test.

Figure 13 shows the gas-phase concentration profiles of O_3, SO_2, H_2O_2, HNO_3, and sulfate after 1 h of cloud simulation with the CTM cloud module using the MM4 data (72-h forecast) of the KUO, WARM, KUO + WARM, COLD, and KUO + COLD simulations. The most significant differences occur in the levels above cloud top and in the levels below cloud base and where the liquid water content has its maximum value.

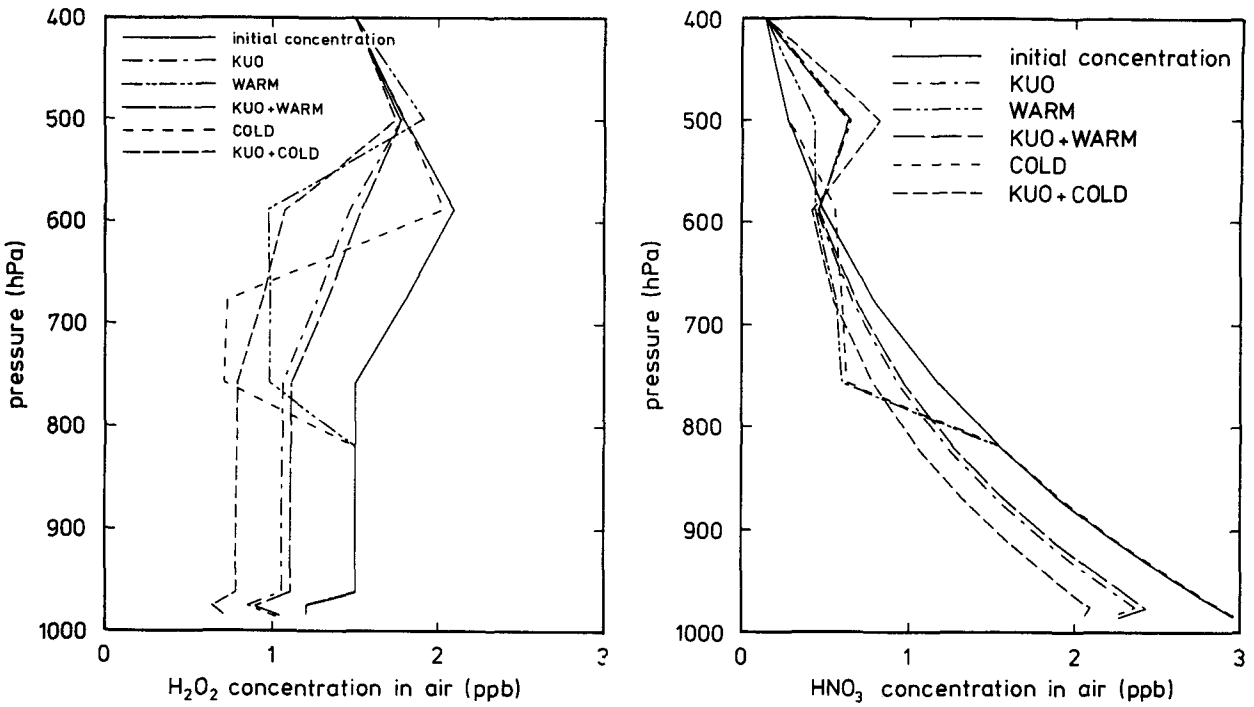

FIG. 13. (*Continued*)

The differences in the concentrations above the clouds are caused by entrainment (Fig. 13). The calculated concentration profiles shown in Fig. 13 also evidence the influence of cloud top and cloud base on the gas phase distributions. Note that in the case of the KUO + COLD run the sulfate gas-phase concentration is higher than the initial concentration (Fig. 13). It seems that in this case the sulfate production is higher than the loss by washout. This is manifested by the large decrease of H_2O_2 and SO_2 concentrations in air, which is strongest for the KUO + COLD run. But there are also cases where the loss by washout and/or the dilution by entrainment are larger than the sulfate production. Thus, in such cases the sulfate concentration in air after 1 h of simulation would be lower than the initial concentration. In contrast to sulfate, HNO_3 has no production term in this stand-alone version of the CTM cloud package and, hence, the concentrations are only changed by entrainment and washout.

The wet deposition strongly varies between the tests depending on the cloud cover, cloud extension, and position of cloud base and top diagnosed by the CTM cloud module as well as on the rain rate predicted by MM4 (see also Table 2). The studies show that the largest differences in wet deposition are caused by differences in cloud cover and rain rate. Discrepancies due to different cloud extensions were mostly found not to be as significant for the calculated wet deposition as those caused by others.

6. Conclusions

MM4 has been run using five different cloud modules: cumulus parameterization scheme (KUO), warm scheme (WARM), ice parameterization scheme (COLD), warm scheme, and cumulus parameterization scheme (KUO + WARM), as well as ice and cumulus parameterization (KUO + COLD).

Although strong convection occurred during the simulated episode and the runs were performed for a horizontal resolution of 80 km × 80 km, which is more appropriate for the KUO simulation, in our case studies the ice parameterization (COLD) provided the best forecast for the precipitation and the moisture fields.

The warm scheme, which provided satisfactory results in case studies with moderate weather conditions (e.g., Hsie and Anthes 1984), seems to be overload to simulate weather conditions where deep convection with ice topped clouds occurs. Hence, the inclusion of ice microphysics (COLD simulation) contributes to improved forecasts.

From the physical point of view the KUO + COLD should perform the best. This is false, however, because the two parameterization schemes used together in MM4 compete for the available moisture, where, in contrast to the ice parameterization scheme, the cumulus parameterization scheme does not consider cloud water, rainwater, or ice. Our case studies evidence that it is not reasonable or advantageous to combine the cumulus parameterization scheme with the warm

scheme or the cumulus parameterization scheme with the ice parameterization scheme without major modifications to the cumulus parameterization with respect to cloud water, rainwater, and ice.

The meteorological data after 72 h of forecast have been used as input data for the CTM cloud module to illustrate the inconsistencies in the treatment of clouds in MM4 and CTM and its consequences for the trace gas distributions and the wet deposition. The studies have illustrated that calculated wet deposition rates vary strongly for the five tests. The main reasons are the differences in the precipitation rates and in the cloud cover. The discrepancies due to different cloud extensions seem to be not as significant for the calculated wet deposition as those caused by the others.

The precipitation amount and the cloud cover are the most critical parameters for all simulations. The largest differences are found in the precipitation amounts. Although in MM4 the horizontal cloud distribution was predicted best by the COLD simulation, the cloud cover rediagnosed by the CTM cloud module is the best for the tests with the data of the KUO simulation because the CTM cloud cover parameterization [Eq. (29)] was developed for this cloud module combination (MM4 with cumulus parameterization and CTM cloud module).

The heights of the cloud base and the cloud top vary strongly depending on the MM4 cloud module chosen, and are not the same for CTM and MM4. This causes differences in photolysis rates, in aqueous- and gas-phase chemistry as well as in the wet deposition rates. The inconsistencies between the cloud extensions predicted in MM4 and CTM limit the confidence, especially in the predicted concentration distributions and the calculated deposition.

All cloud water, rainwater, and ice (if included) predicted by MM4 are neglected by CTM. This seems to be physically doubtful, as the atmosphere is dried artificially. Such a procedure leads to an unfounded loss of water in the hydrological cycle. Therefore, the large amounts of water and ice should not be neglected (and will be included in CTM in future modeling).

The discrepancies in the results provided by the inconsistent cloud modules in MM4 and CTM cause problems in the argument for the use of different cloud modules within the EURAD model architecture and, moreover, aggravate the interpretation of the results.

Our investigations have shown that the calculated concentration fields and deposition rates can strongly depend on the model architecture. The discrepancies in the cloud simulation in CTM and MM4 are the smallest when the cumulus parameterization is used in MM4 as the CTM cloud module is then (more or less) similar to that of MM4. This fact suggests that the performance of the EURAD model package can be improved if the treatment of the clouds in MM4 and CTM is consistent. If a new cloud module should be used in MM4, the CTM cloud module must (be readjusted or better) be the same as the MM4 cloud module with some additional options to determine those parameters that are necessary in CTM but are not calculated by the MM4 cloud module, for example, cloud cover. The parameterization of the cloud cover should consider overlapping of clouds like the parameterization proposed by Sundqvist et al. (1989). (Note that the warm scheme and the ice parameterization scheme in MM4 already predict clouds in different atmospheric layers.) A cloud module package achieving consistency between the cloud simulation in MM4 and CTM and considering the requirements mentioned above is under development.

Acknowledgments. We are grateful to M. P. Scheele and G. H. L. Verver from the KNMI (Koninklijk Nederlands Meteorologisch Instituut) who gave access to the precipitation data. We gratefully acknowledge the support from U. Steffens and E. Raschke from the Institut für Geophysik und Meteorologie der Universität zu Köln in data processing of the *NOAA-9* satellite data. We should like to express our thanks also to G. Kramm from the Fraunhofer-Institut für Atmosphärische Umweltforschung, to R. Koenig, the editor of the *Journal of Applied Meteorology,* and the anonymous reviewers for fruitful discussions, helpful comments, and critical questions. Computational support was performed by the Research Center Jülich (KFA), in particular by ICH2 and ICH3. This work was funded by the Ministry of Research and Technology (BMFT) of Germany and from the Ministry of Science and Research of NRW (Ministerium für Wissenschaft und Forschung des Landes Nordrhein-Westfalen).

REFERENCES

Anthes, R. A., 1977: A cumulus parameterization scheme utilizing a one-dimensional cloud model. *Mon. Wea. Rev.*, **107**, 963–984.

——, E.-Y. Hsie, and Y.-H. Kuo, 1987: Description of the Penn State/NCAR Mesoscale Model Version 4 (MM4), NCAR/TN-282 + STR. [Available from Publication Office, NCAR, P.O. Box 3000, Boulder, CO 80307-3000.]

Asai, T., 1965: A numerical study of air-mass transformation over the Japan sea in winter. *J. Meteor. Soc. Japan,* **43**, 1–15.

Chang, J. S., R. A. Brost, I. S. A. Isaksen, S. Madronich, P. Middleton, W. R. Stockwell, and C. J. Walcek, 1987: A three-dimensional Eulerian acid deposition model: Physical concepts and formulation. *J. Geophys. Res.*, **92**, 14 681–14 700.

Chang, T. Y., 1984: Rain scavenging of HNO_3-vapor in the atmosphere. *Atmos. Environ.*, **18**, 191–197.

Cotton, W. R., M. A. Stephens, T. Nehrkorn, and G. J. Tripoli, 1982: The Colorado State University three-dimensional cloud mesoscale model 1982. Part II: An ice phase parameterization. *J. Rech. Atmos.*, **16**, 295–320.

——, G. J. Tripoli, R. M. Rauber, and E. A. Mulvihill, 1986: Numerical simulations of the effects of varying ice crystal nucleation rates and aggregation processes on orographic snowfall. *J. Climate Appl. Meteor.*, **25**, 1658–1680.

Dudhia, J., 1989: Numerical study of convection observed during the winter monsoon experiment using a mesoscale two-dimensional model. *J. Atmos. Sci.*, **46**, 3077–3106.

Fletcher, N. H., 1962: *The Physics of Rain Clouds.* Cambridge University Press, 386 pp.

Hass, H., M. Memmesheimer, H. Geiß, H. J. Jakobs, M. Laube, and A. Ebel, 1990: Simulation of the Chernobyl radioactive cloud over Europe using the EURAD model. *Atmos. Environ.*, **24,** 673–692.

——, A. Ebel, H. Feldmann, H. J. Jakobs, and M. Memmesheimer, 1993: Evaluation studies with a regional chemical transport model (EURAD) using air quality data from EMEP monitoring network. *Atmos. Environ.*, **27A,** 867–889.

Hsie, E.-Y., and R. A. Anthes, 1984: Simulations of frontogenesis in a moist atmosphere using alternative parameterizations of condensation and precipitation. *J. Atmos. Sci.*, **41,** 2701–2716.

Kessler, E., III, 1969: *On the Distribution and Continuity of Water Substance in Atmospheric Circulations. Meteor. Monogr.*, No. **32,** Amer. Meteor. Soc., 84 pp.

Kuo, H. L., 1974: Further studies of the parameterization of the influence of cumulus convection on large-scale flow. *J. Atmos. Sci.*, **31,** 1232–1240.

Lin, Y.-L., R. D. Farley, and H. D. Orville, 1983: Bulk parameterization of the snow field in a cloud model. *J. Climate Appl. Meteor.*, **22,** 1065–1092.

Locatelli, J. D., and P. Hobbs, 1974: Fall speeds and masses of solid precipitation particles. *J. Geophys. Res.*, **79,** 2185–2197.

Lord, S. J., H. E. Willoughby, and J. M. Piotrowicz, 1984: Role of parameterized ice-phase microphysics in an axisymmetric, nonhydrostatic tropical cyclone model. *J. Atmos. Sci.*, **41,** 2836–2848.

Marshall, J. S., and W. M. Palmer, 1948: The distribution of raindrops with size. *J. Meteor.*, **5,** 165–166.

Memmesheimer, M., J. Tippke, A. Ebel, H. Hass, H. J. Jakobs, and M. Laube, 1991: On the use of EMEP emission inventories for European scale air pollution modelling with the EURAD model. *EMEP workshop on photooxidant modelling for long-range transport in relation to abatement strategies,* EMEP, Berlin, F.R.G., 307–324.

Meyers, M. P., P. J. DeMott, and W. R. Cotton, 1992: New primary ice-nucleation parameterizations in an explicit cloud model. *J. Appl. Meteor.*, **31,** 708–721.

Orville, H. D., and F. J. Kopp, 1977: Numerical simulation of the life history of a hailstorm. *J. Atmos. Sci.*, **34,** 1596–1618.

Pruppacher, H. R., and J. D. Klett, 1980: *Microphysics of Clouds and Precipitation,* Reidel Publishing Company, 714 pp.

Scott, B. C., 1981: Sulfate washout in winter storms. *J. Appl. Meteor.*, **20,** 619–625.

Sundqvist, H., E. Berge, and J. E. Kristjansson, 1989: Condensation and cloud parameterization studies with a mesoscale numerical weather prediction model. *Mon. Wea. Rev.*, **117,** 1641–1657.

Topol, L. E., 1986: Differences in ionic compositions and behavior in winter rain and snow. *Atmos. Environ.*, **20,** 347–355.

Walcek, C. J., and G. R. Taylor, 1986: A theoretical method for computing vertical distributions of acidity and sulfate production within cumulus clouds. *J. Atmos. Sci.*, **43,** 339–355.

Zhang, D.-L., 1989: The effect of parameterized ice microphysics on the simulation of vortex circulation with a mesoscale hydrostatic model. *Tellus,* **41A,** 132–147.

Zikmunda, J., and B. Vali, 1972: Fall patterns and fall velocities of rimed ice crystals. *J. Atmos. Sci.*, **29,** 1334–1347.